1 Introduction

We are witnessing a new generation of applications of thin film transistors (TFTs) for flat-panel imaging [1, 2, 3] and displays [4, 5, 6]. Unlike the active matrix liquid crystal display (AMLCD) where the TFT acts as a simple switch [7], new application areas are emerging, placing demands on the TFT to provide analog functions including managing instability arising from material disorder [3, 6].

In the following sections, we briefly describe the application platforms we have considered in this book, namely flat-panel displays and imaging, along with a summary of performance characteristics of the key TFT technologies used, or being considered, by the large-area electronics industry. While the circuit architectures reported here use examples based on amorphous silicon technology, they are easily adaptable to a broad range of materials families and applications with different specifications.

1.1 Organic light emitting diode displays

OLEDs have demonstrated promising features to provide high-resolution, potentially low-cost, and wide-viewing angle displays. More importantly, OLEDs require a small current to emit light along with a very low operating voltage (3–10 V), leading to very power efficient light emitting devices [4–6].

OLEDs are fabricated either by organic (small molecule) or polymeric (long molecule) materials. Small molecule OLEDs are produced by an evaporation technique in a high vacuum environment [8],

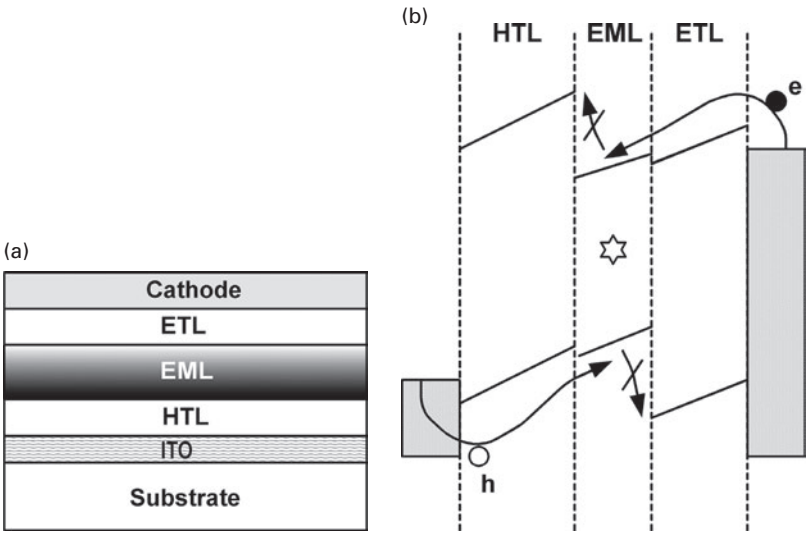

Figure 1.1 Multi-layer OLED stack structure and (b) OLED banding diagram adapted from [8, 10].

whereas, polymeric OLEDs are fabricated by spin-coating or inkjet printing [9]. However, the efficiency of small molecule OLEDs is much higher than that of polymeric OLEDs.

To increase the efficiency of the OLED, an engineered band structure is adopted [8]. A typical multi-layer OLED and its corresponding banding diagram are illustrated in Figure 1.1. The indium tin oxide (ITO) layer is the anode contact. The hole-transport layer (HTL), a p-doped layer, provides holes for the emission layer (EML), and also prevents electrons from traveling to the anode because of the band offset with the adjacent layers. For the cathode, the electron transport layer, an n-doped layer, provides electrons for the EML, and prevents the holes from traveling to the cathode. Then, the electrons and holes are recombined in the EML layer, resulting in the generation of photons [8, 10].

The luminance of OLEDs is linearly proportional to their current at low-to-mid current densities, and saturates at higher current densities.

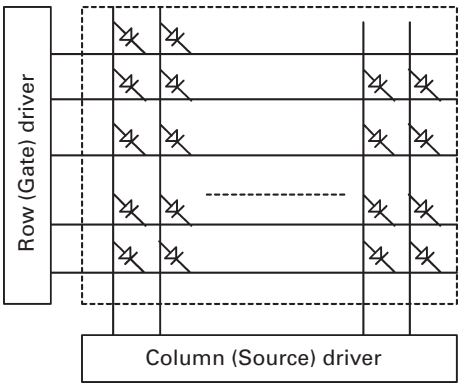

Figure 1.2 Passive matrix OLED display structure adapted from [16].

However, the voltage of OLEDs increases over time due to crystallization, chemical reaction at the boundaries, changes in the charge profile of the layer, and oxidation due to the existence of oxygen and moisture [11, 13]. Consequently, most of the proposed driving schemes are designed to provide a constant current for OLEDs.

OLEDs offer great promise in either passive or active formats. Figure 1.2 portrays passive matrix OLED (PMOLED) architecture. By applying a voltage across the appropriate row and column contacts, a specific pixel is addressed. Thereby, a current flows through the organic layers at the intersection of these contacts to light up the pixel. In this architecture, the luminance during the programming is averaged for the entire frame rate. Thus, the pixel should be programmed for $N \times L$ where N is the number of rows and L is the desired luminance for a frame [15, 16]. Thus, the OLED current density increases significantly, especially for higher resolution displays [5, 17]. Since the OLED efficiency drops at high current densities [18], to increase the display resolution, the current increases by a power law instead of linearly. Thus, the power consumption increases and the OLED ages faster. As a result, the actual applications of PMOLED displays are limited to small displays that have a low resolution [5].

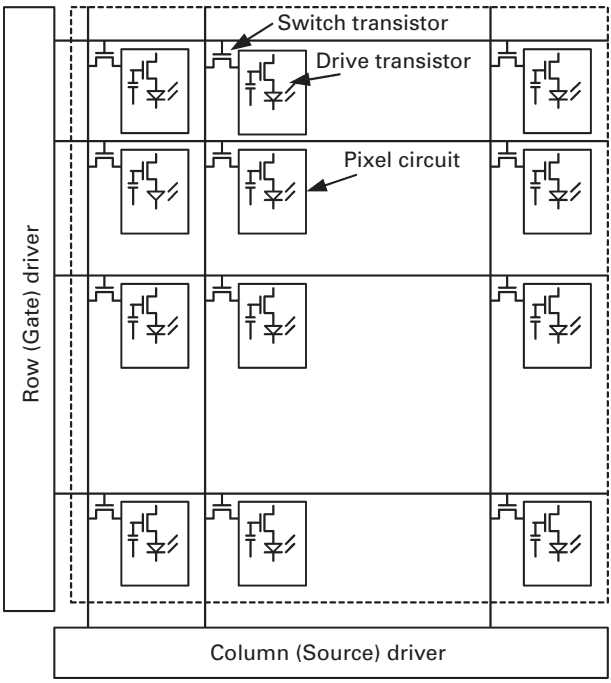

Figure 1.3 Active matrix OLED (AMOLED) display structure.

To increase the resolution and area of the displays, active matrix addressing is selected [5]. A simplified active matrix OLED (AMOLED) display structure is illustrated in Figure 1.3, where the pixel current is controlled by a drive transistor. During the programming cycle, the switch TFT is ON, and the pixel data is stored in the storage capacitor. During the driving cycle, a current, related to the stored data voltage, is provided to the OLED. Since the pixel current is smaller in the AMOLED displays, they have longer lifetimes than PMOLED displays.

Figure 1.4(a) reflects the structure of a bottom-emission AMOLED display in which the light passes through the substrate [19]. Thus the substrate is limited to transparent materials, and the aperture ratio is diminished by the area lost to the pixel circuitry, resulting in a higher current density. Moreover, the aperture ratio becomes more critical when considering a more complex pixel

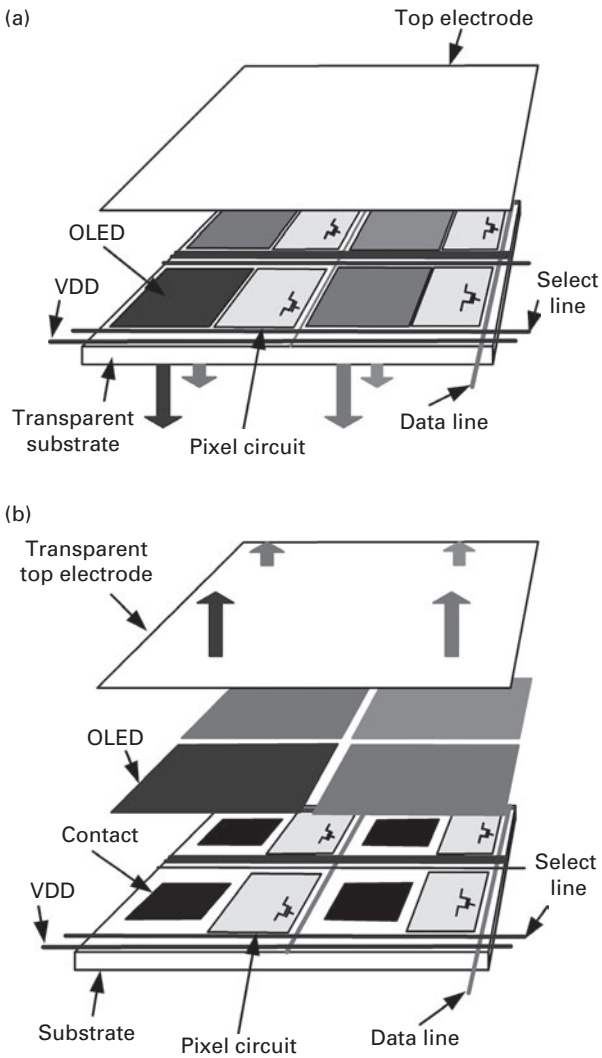

Figure 1.4 Bottom and top emission AMOLED pixel structure. Color versions of these figures are available online at www.cambridge.org/chajinathan.

circuit to compensate for both spatial and temporal non-uniformities. Hence, top-emission displays are preferred (see Figure 1.4(b)). It provides for more than an 80% aperture ratio, and the substrate is not required to be transparent [20].

1.2 Flat-panel biomedical imagers

Large-area flat-panel digital imaging has been valued for its advantages, including the separation of detector, image storage, and display, which facilitates independent improvement by isolating the complexity of the different parts from each other. Moreover, it enables the use of digital processing of the captured images to improve visual quality and to make feasible the use of computer-aided diagnostics [2, 21, 22]. The basic blocks of a flat-panel imager include a sensor and a readout circuitry using transistors which act either as a switch or as an amplifier. The sensor, commonly used in these applications, is a PIN or a MIS diode in the case of indirect detection (in which X-rays are converted to optical signals by phosphor layers) or amorphous selenium for direct detection (whereby the incident X-rays are directly converted to electrical charge).

Figure 1.5 shows a passive pixel sensor (PPS) architecture in which the pixel consists of a switch TFT and a capacitor. The charge generated by the sensor is integrated into the storage capacitor, which is read out by a charge-pump amplifier, while the switch TFT is ON. The gain of the PPS pixel is given as

$$V_{out} = Qt_{int}C_g. \tag{1.1}$$

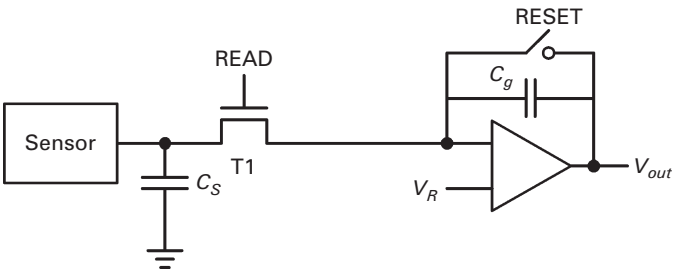

Figure 1.5 PPS imager pixel circuit adapted from [1, 2].

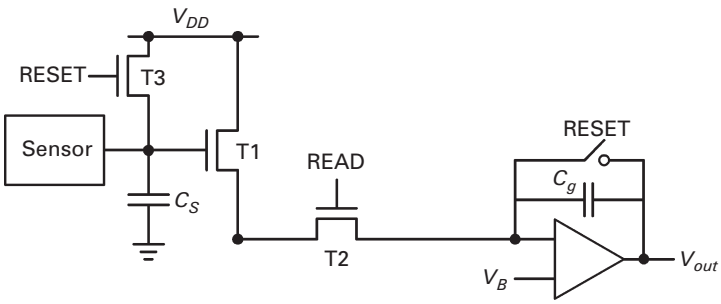

Figure 1.6 3-TFT APS imager pixel circuit adapted after [3].

Here, Q is the charge generated by the sensor and t_{int} the integration time. However, due to non-uniformities such as noise and leakage currents, the minimum level, detectable by PPS pixel, is limited.

To improve the sensitivity to small intensity signals, an active pixel sensor (APS) was introduced by Matsuura [3] (see Figure 1.6). Here, the storage capacitor is charged to a reset voltage. Then, the collected sensor charge into the storage capacitor modulates the current of the amplifier TFT (T1) as

$$I_{px} = g_m Q t_{int} \quad \text{and} \quad V_{out} = C_g I_{px} t_{read}, \tag{1.2}$$

in which g_m is the trans-conductance of T1, and t_{read} the time associated with the readout cycle. However, for high-intensity input signals, the on-pixel gain saturates the readout circuitry. In particular, for biomedical X-ray imaging applications, the significant contrast in the signal intensity of the different imaging modalities mandates unique pixel design.

Recently, hybrid mode pixel circuits have been reported that can operate between the passive and active readout for modalities employing high and low X-ray intensities, respectively. Figure 1.7 shows the 3-TFT hybrid pixel circuit presented in [23]. The issue with this type of a circuit is that it can be optimized for only active or passive operation. For example, in the active readout mode, a small storage pixel is required to improve the SNR [23], whereas, in the passive readout, a

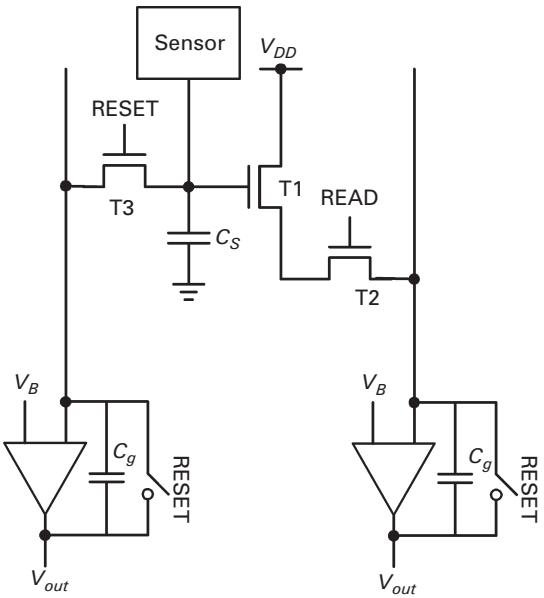

Figure 1.7 Hybrid active-passive imager pixel circuit adapted from [23].

large storage capacitor is needed to avoid saturation, improving the maximum detectable signal intensity. Also, a high-resolution (2-TFT) version of this pixel has been reported [24]. In addition to a limited dynamic range, this circuit suffers from cross talk and accelerated aging of TFTs. In particular, during the readout cycle of a row, the amp TFTs in pixels of inactivated rows are in the linear regime resulting in relatively high cross talk and accentuated aging [25]. Moreover, to achieve linear sensitivity, the amplifier TFT is biased in the linear regime, which makes it very susceptible to IR drop and ground bouncing.

1.3 Backplane technologies

The pixel circuits discussed above can be fabricated using different technologies, notably, poly silicon (poly-Si) [27, 28, 29] and hydrogenated amorphous silicon (a-Si:H) [3, 6, 30]. Poly-Si technology

Table 1.1 *Comparison of TFT backplane technologies for large-area electronics [26].*

Attribute	a-Si:H	Oxide	Poly-Si	mc/nc-Si:H	Organic
Circuit type	n-type	n-type	n-type/p-type	n-type/p-type	p-type
Mobility ($cm^2/V\,s$)	< 1	~10	10~100	~1 to 10	$<< 1$
Temporal stability (ΔV_T)	issue	more stable than a-Si:H	more stable than a-Si:H	more stable than a-Si:H	improving
Initial uniformity	high	higher than poly-Si	low	potentially high	low
Manufacturability	mature	developing	developing	research	reseach
Cost	low	low	high	low	potentially low

offers high-mobility and complementary (n-type and p-type) TFTs [28, 29], but has an undesirable large range of mismatched parameters over an array [31, 32]. This is due to the random distribution of the grain boundary in the material [31].

In contrast, a-Si:H provides low mobility TFTs but does not provide p-type devices [33]. Also, the threshold voltage of TFTs increases (V_T-shift) under prolonged bias stress due to the inherent instability of a-Si:H material [34, 35]. Despite this, the technology provides good uniformity over a large area. More importantly, a-Si:H technology's industrial accessibility, by virtue of its usage in the AMLCD [7], provides for low-cost large-area electronics. In particular, an a-Si:H TFT backplane has the benefit of all the desirable attributes of the well-established a-Si:H technology, including low-temperature fabrication on plastic for eventual flexible electronics. Table 1.1 lists the attributes of different possible fabrication technologies.

In addition, promising research is being carried out on new materials such as hydrogenated nano/micro crystalline (nc/mc) silicon [36, 37, 38], organic semiconductors [39, 40], and more recently, the highly promising amorphous oxide semiconductors [41–43]. The nc/mc-Si:H and oxide semiconductor (e.g. indium gallium zinc oxide) technologies provide higher temporal stability (see [37, 38, 44–47] and references therein) and mobility (see [36, 43, 44, 47, 48] and references therein) compared to the ubiquitous a-Si:H technology. However, light-induced instability can be an issue [45, 46] requiring special driving techniques for threshold-voltage recovery [45, 47]. Despite this a variety of analog and digital circuits have been demonstrated [49, 50], including active matrix organic displays [51, 57] and imaging arrays [47, 52, 53]. On the other hand, an organic semiconductor has the potential for extremely low cost fabrication, including inkjet printing. However, this technology suffers from bias-induced [41, 42, 54–56] and environment-induced instabilities [43] and poor uniformity [44].